Determination of Nerve Agent Metabolites by Ultraviolet Femtosecond Laser Ionization Mass Spectrometry

Hamachi, Akifumi
Department of Applied Chemistry, Graduate School of Engineering, Kyushu University

Imasaka, Tomoko
Laboratory of Chemistry, Graduate School of Design, Kyushu University

Nakamura, Hiroshi
Division of International Strategy, Center of Future Chemistry, Kyushu University

Li, Adan
Division of International Strategy, Center of Future Chemistry, Kyushu University

他

出版情報：Analytical chemistry. 89 (9), pp.5030-5035, 2017-05-02. American Chemical Society
バージョン：
権利関係：

Determination of Nerve Agent Metabolites by Ultraviolet Femtosecond Laser Ionization Mass Spectrometry

Akifumi Hamachi,[†] Tomoko Imasaka,[§] Hiroshi Nakamura,[#] Adan Li,[#] and Totaro Imasaka[#]*

[†]*Department of Applied Chemistry, Graduate School of Engineering, Kyushu University, 744 Motooka, Nishi-ku, Fukuoka 819-0395, Japan*

[§]*Laboratory of Chemistry, Graduate School of Design, Kyushu University, 4-9-1 Shiobaru, Minami-ku, Fukuoka 815-8540, Japan*

[#]*Division of International Strategy, Center of Future Chemistry, Kyushu University, 744 Motooka, Nishi-ku, Fukuoka 819-0395, Japan*

* To whom correspondence should be addressed. E-mail: imasaka@cstf.kyushu-u.ac.jp

ABSTRACT

Nerve agent metabolites, i.e., isopropyl methylphosphonic acid (IMPA) and pinacolyl methylphosphonic acid (PMPA), were derivatized by reacting them with 2,3,4,5,6-pentafluorobenzyl bromide (PFBBr) and were determined by mass spectrometry using an ultraviolet femtosecond laser emitting at 267 and 200 nm as the ionization source. The analytes of the derivatized compounds, i.e., IMPA-PFB and PMPA-PFB, contain a large side-chain, and molecular ions are very weak or absent in electron ionization mass spectrometry. The use of ultraviolet femtosecond laser ionization mass spectrometry, however, resulted in the formation of a molecular ion, even for compounds such as these that contain a highly-bulky functional group. The signal intensity was larger at 200 nm due to resonance-enhanced two-photon ionization. In contrast, fragmentation was suppressed at 267 nm (non-resonant two-photon ionization) especially for PMPA-PFB, thus resulting in a lower background signal. This favorable result can be explained by the small excess energy in ionization at 267 nm and by the low-frequency vibrational mode of a bulky trimethylpropyl group in PMPA.

Nerve agents for use in warfare were developed before and during World War II and are known to be extremely toxic for humans.[1-3] The development, manufacture, stockpiling, and use of these compounds are prohibited by the Convention on the Prohibition established by the Organization for the Prohibition of Chemical Weapons (OPCW).[4] The most well-known nerve agents are sarin, soman, and VX gases, and have been used by various terrorist organizations and even by nations. Nerve agents undergo decomposition in the human body, with the formation of intermediates which then dissociate into final products, as shown in Fig. 1.[5] For example, sarin and soman lose a fluorine atom and are converted into isopropyl methylphosphonic acid (IMPA) and pinacolyl methylphosphonic acid (PMPA), respectively. The alkyl groups are subsequently released and are converted into methylphosphonic acid (MPA). If a nerve agent has been used, it can be identified by measuring metabolites produced from it in a body fluid such as urine.

A sensitive and selective analytical method is needed to measure trace species in an actual sample that would also contain a variety of interfering species. Matrix-assisted laser desorption ionization mass spectrometry (MALDI-MS) provides a molecular or pseudo-molecular ion and has been utilized for direct determination of nerve agent metabolites.[6] Mass spectrometry (MS) combined with a separation technique such as gas chromatography (GC) or liquid chromatography (LC) has superior selectivity and been successfully used for the determination of these compompounds.[2,3,5,7] A combination of GC and MS (GC/MS) is in particularly widespread use for this purpose.[5,7,8] However, most nerve agent metabolites contain some highly polar functional groups. For this reason, they need to be derivatized with a chemical reagent for vaporization prior to GC/MS analysis. A variety of derivatization reagents have been developed and used for the determination of nerve agent metabolites, which are summarized in a review article.[8] Structurally-informative high-mass ions including a molecular or quasi-molecular ion are preferable

for trace analysis. However, a finger-printing fragment pattern is also necessary for the identification of the compounds. Silylation and esterification are the most frequently used techniques for derivatization.[3,8] Unfortunately, electron ionization (EI), which is currently used in MS, provides no molecular ion for the derivatized compounds.[9] It should be noted that nerve agents such as sarin and soman contain similar functional groups and their fragment patterns are similar. Positive ion chemical ionization (PICI) provides a few adduct ions,[10] making the MS spectrum more complicated. Although negative ion chemical ionization (NICI) provides a single peak for a compound corresponding to the dissociation products (IMPA and PMPA), the identification of the nerve agent is not reliable due to a lack of fragmentation patterns.[9] To address this issue, more complicated technique such as GC/MS-MS can be utilized,[10,11] which, however, makes a comprehensive analysis difficult. Then, it would be desirable to develop a comprehensive MS technique that produces a molecular ion as well as several fragment ions for a structurally informative and reliable trace analysis of the target molecule, as well as unknown nerve agent metabolites with similar chemical structures.

Photoionization MS is one of the advanced techniques available for observing a molecular ion.[12] Indeed, femtosecond ionization mass spectrometry (FI-MS) has been utilized for the analysis of organic compounds such as dioxins, pesticides, and even explosives.[13-15] This technique is useful for improving ionization efficiency by means of resonance-enhanced multiphoton ionization (REMPI), in which a molecule can be excited to a singlet excited state by absorbing the first photon and subsequently ionized by absorbing additional photons. Ionization efficiency increases when the laser wavelength coincides with the energy of excitation. In addition, a femtosecond laser can be employed for efficient ionization before intersystem crossing to triplet levels. Because of this, FI-MS retains a high efficiency of ionization even for a molecule that contains multiple halogen

atoms or even a nitro group, when the laser pulse width is shorter than the lifetime of the excited state.[16-18] However, because there are many types of organic compounds in the environment, the performance of FI-MS should be examined using a variety of compounds with different properties. Numerous allergenic compounds contained in fragrances, which consist of many types of aromatic/aliphatic hydrocarbons with/without ring/non-ring, conjugated/non-conjugated double-bonds, and/or short/long side chains, have been measured.[19] The FI-MS technique generally provides a molecular ion and is more reliable than EI-MS. However, applying FI-MS to different types of compounds to examine the advantage and the limitation of this technique represents a real challenge.

In this study, we report on the measurement of IMPA and PMPA, metabolites of sarin and soman, after derivatization, since a novel analytical methodology is required for homeland security. It should be noted that the molecular ions for such compounds are very weak or nonexistent when measured using EI-MS, probably due to the presence of a bulky side-chain such as an isopropyl or pinacolyl group in the molecule (see Fig. 1 (A)). Indeed, the fragment patterns are very similar to each other, although a few MS peaks can be used for identification.[9] Thus, an MS technique that would provide a molecular ion would be useful, not only for identifying the compound but also for suppressing interfering species with low molecular weights. A femtosecond laser emitting at 200 nm (far-ultraviolet, FUV) and at 267 nm (deep-ultraviolet, DUV) was evaluated as an ionization source. To our knowledge, this is the first study reporting the determination of nerve agent metabolites using FI-MS. We discuss the advantage of this technique and also the limitations that need to be solved in the future.

EXPERIMENTAL SECTION

Sample. The nerve agent metabolites, IMPA and PMPA, were derivatized with 2,3,4,5,6-pentafluorobenzyl bromide (PFBBr), as shown in Fig. 1 (B). Details of the procedures used have been reported elsewhere,[20] and a simplified protocol shown below was used in this study. A solution containing 10-100 ng of IMPA (1 mg/mL in methanol, Sigma Aldrich Japan, Tokyo, Japan) and PMPA (1 mg/mL in methanol, Sigma-Aldrich Japan) was vaporized under a stream of nitrogen gas, and acetonitrile (600 μL, Wako Pure Chemical Industries, Tokyo, Japan) was added to dissolve these compounds. The derivatization reagent, PFBBr (10 μL, 1 mg/mL, Sigma-Aldrich Japan), and a base, K_2CO_3 (20 mg, Wako Pure Chemical Industries), were added to the sample solution which was then heated at 90 °C for 45 min. The solvent was vaporized using a stream of nitrogen gas and the residue was dissolved in dichloromethane (300 μL, Wako Pure Chemical Industry). The sample solution was passed through a separation column (Bond-Elut Florisil, Agilent Technologies, Santa Clara, CA. USA). A solvent mixture (750 μL) consisting of methanol (10%, Wako Pure Chemical industry) and dichloromethane (90%, Wako Pure Chemical Industry) was passed through the column to elute the analytes, and this procedure was repeated again. The solvent was vaporized to dryness, and the analytes were dissolved in dichloromethane (100 μL). This solution was used as the sample.

Analytical Instrumentation. A sample solution containing nerve agent metabolites was injected into a GC (6890N, Agilent Technologies) interfaced with a time-of-flight mass spectrometer (TOFMS) developed in this laboratory (HK-1, Hikari-GK, Fukuoka, Japan).[17] The third harmonic (267 nm, 25 μJ) and fourth harmonic (200 nm, 6 μJ) emissions of a Ti:sapphire laser (800 nm, 35 fs, 4 mJ, 1 kHz, Elite, Coherent, Santa Clara, CA, USA) was used as the ionization source.[21] A capillary column (DB-5ms, 30 m long, 0.25 mm i.d., 0.25 mm film thickness, Agilent Technologies) was used to separate the IMPA-PFB and PMPA-PFB from side-reaction products.

The temperature of the GC oven was set at 40 °C and held for 5 min, and was then programmed to increase at a rate of 10 °C/min to 280 °C, with a final hold of 1 min. The flow rate of helium, used as the carrier gas, was 1 mL/min. The analytes from the capillary column were introduced into the MS, and the induced ions were accelerated into a flight tube for mass analysis. The signal from an assembly of microchannel plates (MCP) (F4655-11, Hamamatsu Photonics, Shizuoka, Japan) was recorded by a digitizer (AP240, Agilent Technology), which was further processed by a home-made software using LabVIEW, ORIGIN, and Visual Basic.

Quantum Chemical Calculations. The spectral properties of several nerve agents, e.g., sarin, soman, and their metabolites such as IMPA and PMPA, have been calculated and reported elsewhere.[22] In the present study, the spectral properties of IMPA-PFB and PMPA-PFB, the corresponding analytes derivatized with PFBBr, were evaluated based on quantum chemical calculations to examine the ionization mechanism. The optimized geometry of the ground state and the harmonic frequencies were calculated using the B3LYP method,[23] based on density functional theory (DFT) with a cc-pVDZ basis set.[24] The lowest 40 singlet transition energies and their oscillator strengths were calculated using time-dependent DFT (TD-DFT) at the level of B3LYP/cc-PVTZ.[25,26] The predicted absorption spectra were obtained by assuming a Gaussian profile with a half width at half maximum of 0.333 eV. The vertical ionization energy (*IE*) and its half value (*IE*/2) at the level of B3LYP/cc-pVTZ were also calculated from the difference between the energies of the ground and ionic states.

RESULTS AND DISCUSSION

Spectral Properties. The calculated absorption spectra of IMPA-PFB and PMPA-PFB are shown in Fig. 2. An absorption band, referred to as the B-band for benzene derivatives, appears at

around 250 nm, which originates from the functional group of PFB. The molar absorptivity is, however, small due to the forbidden nature of the transition. In contrast, absorption bands at slightly below 200 nm, referred to as the E- and K-bands, are much larger due to their allowed transitions. The analyte molecule would be expected to be excited and efficiently ionized at 200 nm through a process of REMPI, which is in contrast to non-resonant multiphoton ionization (NRMPI) at 267 nm. The calculated ionization energy was 9.25 eV (134.0 nm; *IE*/2, 268.0 nm) for IMPA-PFB and 9.05 eV (137.0 nm; *IE*/2, 274.0 nm) for PMPA-PFB. These molecules are then two-photon ionized (TPI) both at 200 nm (6.20 eV) and 267 nm (4.64 eV). For these reasons, the analyte molecule would be ionized more efficiently at 200 nm, although fragmentation would be more extensive due to a larger excess energy in ionization.

IMPA. The mass spectrum measured for IMPA-PFB at 267 nm is shown in Fig. 3 (A). A molecular ion peak was clearly observed at *m/z* = 318 even under non-resonant two-photon ionization (NRTPI). In addition, several intense fragment ions appeared in the MS. Side-chains such as $-CH_3$, $-C(CH_3)_2$ readily undergo dissociation to form fragment ions of $[M\text{-}CH_3]^+$ and $[M\text{-}C(CH_3)_2]^+$ at *m/z* = 303 and 276, respectively. The ion was further stabilized by dissociating HF (*m/z* = 256). The ions observed at *m/z* = 181 and 80 are assigned to fragment ions corresponding to [M-IMPA+H (PFB)]$^+$ and $[O{=}PH(CH_3)(OH)]^+$, respectively. In EI-MS, a molecular ion is very weak or absent,[9,10] although the fragment pattern is similar to the data shown in Fig. 3 (A). A similar result was reported for a silylation product of IMPA measured using EI-TOFMS.[27] Thus, the present method based on DUV-FI has a distinct advantage of providing a molecular ion. A mass chromatogram measured at *m/z* = 318, corresponding to a molecular ion, is shown in Fig. 3 (B). The largest peak at 352 s is assigned to IMPA-PFB. A signal peak arising from interfering species appears very close to the analyte peak. Because of this, a separation technique such as GC is

essential, even for FI- MS. The detection limit achieved using a molecular ion peak was 3 ng/μL.

Figure 3 (C) shows the mass spectrum obtained by adjusting the laser wavelength at 200 nm. Numerous intense fragment peaks were observed in the MS, although the signal intensity of the molecular ion was increased by 4.6 fold. This signal enhancement can be explained by resonant two-photon ionization (RETPI) and a larger molar absorptivity at 200 nm. However, extensive fragmentation occurred when a large excess energy of 3.15 eV (= 6.20 × 2 – 9.25) at 200 nm was used, as expected from the previous section, which is in contrast to 0.03 eV (= 4.64 × 2 – 9.25) at 267 nm. The signal peaks measured at 200 nm appear to be broadened when compared with the data measured at 267 nm (cf. Fig. 3 (A)). This unexpected result can be explained by a space charge effect because numerous fragment ions appeared at 200 nm. In Fig. 3 (D), an intense signal peak arising from IMPA-PFB, in addition to several other peaks arising from interfering species, is observed in the mass chromatogram obtained by monitoring at m/z = 318. Note that the signal peak of IMPA-PFB is partially superimposed with a signal peak arising from an interfering substance. The detection limit was 2 ng/μL, which was slightly better than that obtained at 267 nm, due to a larger ionization efficiency at 200 nm.

Two-dimensional displays measured for IMPA-PFB at 267 and 200 nm are shown in Fig. 4 (A) and (B), respectively. A molecular ion peak is observed at a retention time of 352 s in both of the data sets. The interfering species appearing at 350 s is, however, partially superimposed with a signal of IMPA-PFB. The signal intensity of the interference appearing at an elution time of IMPA-PFB was ca. 10% of the signal arising from IMPA-PFB, which was confirmed by changing the m/z value used in the construction of the mass chromatogram slightly. As shown in Fig. 3 (A), the background (baseline) was nearly zero when measured at 267 nm. The background, however, increased significantly in the case of the MS measured at 200 nm (see Fig. 3 (C)). It is interesting to

note that no or negligible background was observed in the mass chromatogram (see Fig. 3 (D)). Accordingly, the background observed in the MS did not originate from interfering species, e.g., side-reaction products, or poor separation by GC but from the fragment ions that appeared, even at the position of the molecular ion (*m/z* = 318). This unexpected result can be attributed to limitations in the performance of the MCP detector; the signal failed to recover to zero after large signals arising from fragment ions. Indeed, the background signal continued even at *m/z* = 400, as shown in Fig. 3 (C). This represents one of the limitations associated with the use of TOFMS. This unfavorable result arising from a limited dynamic range of MCP could be solved by using a laser with a higher repetition rate, which would also be useful for avoiding the space charge effect described before.

PMPA. A mass spectrum for PMPA-PFB measured at 267 nm is shown in Fig. 5 (A). As shown in the insert, a molecular ion was observed at *m/z* = 360 at a retention time of 415 s. The intensity of the molecular ion was, however, rather small (3 mV) and extensive fragmentation was observed for PMPA-PFB, even at 267 nm. This undesirable result can be explained by the presence of a bulky side chain of $-(CH_3)HC-C(CH_3)_3$, i.e., a trimethylpropyl group, in PMPA; a side chain with a low-frequency vibrational mode can be dissociated easily. As shown in Fig. 5 (B), several large signals, in addition to signals arising from PMPA-PFB, appeared in the mass chromatogram, even though the signal was extracted at the molecular ion (*m/z* = 360). The detection limit achieved using a molecular ion was ca. 100 ng/μL (1.5 ng/μL with a fragment ion at *m/z* = 318).

Figures 5 (C) and (D) show the data observed for a measurement made at 200 nm. Fragmentation was more serious and numerous fragment peaks appeared in the MS (Fig. 5 (C)). Although a molecular ion was observed, as shown in the insert, the signal intensity was low and the baseline level increased significantly; the background was ten times larger than the molecular ion

signal. Note that the background level in the mass chromatogram obtained by monitoring at *m/z* = 360 (Fig. 5 (D)) is negligibly small. As discussed previously, the background signal (baseline increase) in the MS would originate from fragments; most of the signals for PMPA-PFB in the mass chromatogram obtained by monitoring at *m/z* = 360 would originate, not from the molecular ion, but from the fragment ions due to the limited recovery time of the MCP detector as described. The detection limit achieved using a molecular ion was slightly less than ca. 100 ng/μL (0.3 ng/μL with a fragment ion at *m/z* =318).

A two-dimensional display of the region where PMPA-PFB appears is shown in Fig. 6. Two signals with equal intensities are clearly observed in the mass chromatogram obtained by monitoring at *m/z* = 360 (see Fig. 6 (A)). The mass spectra and the signal intensities are very close to each other. This result can be explained by the fact that PMPA is composed of four stereoisomers due to the asymmetric centers at the phosphorus atom and the pinacolyl carbon. These stereoisomers can be separated into two diastereomer pairs with similar retention times and fragment patterns when a conventional (non-chiral) column is used.[9]

Suppression of fragmentation. The molecular ion was observed for both IMPA-PFB and PMPA-PFB in this study. Fragmentation was, however, significant, probably due to the presence of a bulky substituent group in IMPA and PMPA, even when an FUV pulse (200 nm) was used for RETPI. For this reason, the detection limit obtained for IMPA-PFB using a molecular ion was at the level of a few nanograms, similar to that obtained using a fragment ion in EI-MS measured in the full-scan mode.[11,28] Further optimization of the laser wavelength would be expected to minimize the excess energy and suppress fragmentation. Indeed, the DUV pulse (267 nm) was more favorable for suppressing fragmentation. It should be noted that the ionization efficiency in NRTPI can be improved by decreasing the laser pulse width to <100 fs.[29] Then, a shorter laser pulse emitting at

slightly longer wavelengths, e.g., 20 fs and 270-280 nm, would be useful to increase the ionization efficiency and to decrease the excess energy. Cooling an analyte molecule by supersonic jet expansion would be also useful for decreasing the excess energy in the ionized state by decreasing the initial velocity distribution of the molecule in the ground state.[30] Another approach would be the use of a different type of derivatizing reagent. In fact, PFBBr was used in this study, because it has been reported to be useful for volatizing IMPA and PMPA. A derivatization reagent with a higher absorptivity at longer wavelengths would be preferential for efficient RETPI with a minimum excess energy for suppressing fragmentation.

CONCLUSIONS

Nerve agent metabolites of IMPA and PMPA were measured after derivatization with PFBBr by GC/TOFMS using DUV (267 nm) and FUV (200 nm) femtosecond lasers for NRTPI/RETPI. In contrast to the data obtained by EI-MS, molecular ions were observed for FI-MS. The signal intensity of IMPA-PFB was larger when measured at 200 nm, although fragmentation was more serious in the case of FUV ionization. Fragmentation was more serious for PMPA-PFB, due to the presence of a bulky functional group, providing a 10-fold larger background signal arising from the fragments even at an *m/z* corresponding to the molecular ion. As demonstrated, a two-dimensional display provided an excellent tool for visualizing the data to interpret contributions made by interfering substances.

ACKNOWLEDGMENTS

This research was supported by a Grant-in-Aid for Scientific Research from the Japan Society for the Promotion of Science (JSPS KAKENHI Grant Number 26220806, 15K13726, and 15K01227).

The computations were mainly carried out using the computer facilities at the Research Institute for Information Technology, Kyushu University.

REFERENCES

1. Jokanović, M. *Toxicol. Lett.* **2009**, *188*, 1-10.
2. Kim, K.; Tsay, O. G.; Atwood, D. A.; Churchill, D. G. *Chem. Rev.* **2011**, *111*, 5345–5403.
3. Black, R. M.; Read, R. W. *Arch. Toxicol*. **2013**, *87*, 421-437.
4. Convention on the Prohibition of the Development, Production, Stockpiling and Use of Chemical Weapons and on their Destruction, Organisation for the Prohibition of Chemical Weapons (OPCW), https://www.opcw.org/chemical-weapons-convention/
5. Kanamori-Kataoka, M.; Seto, Y. *J. Health Sci.* **2008**, *54*, 513-523.
6. Shu, Y. R.; Su, A. K.; Liu, J. T.; Lin, C. H. *Anal. Chem.* **2006**, *78*, 4697-4701.
7. Capacio, B. R.; Smith, J. R.; Gordon, R. K.; Haigh, J. R.; Barr, J. R.; Lukey, B. J. *Clinical detection of exposure to chemical warfare agents.* In: Romano Jr. J. A.; Lukey, B. J.; Salem, H. (eds) *Chemical warfare agents. Chemistry, pharmacology, toxicology, and therapeutics*; CRC Press: Boca Raton, **2008**, 501-548.
8. Black, R. M.; Muir, B. *J. Chromatogr. A* **2003**, *1000*, 253-281.
9. Shih, M. L.; Smith, J. R.; McMonagle, J. D.; Dolzine, T. W.; Gresham, V. C. *Biol. Mass Spectrom.* **1991**, *20*, 717–723.
10. Fredriksson, S. Å.; Hammarström, L. G.; Henriksson, L.; Lakso, H. Å. *J. Mass Spectrom.* **1995**, *30*, 1133–1143.
11. Riches, J.; Morton, I.; Read, R. W.; Black, R. M. *J. Chromatogr. B* **2005**, *816*, 251-258.
12. Boesl, U.; Zimmermann, R.; Weickhardt, C.; Lenoir, D.; Schramm, D. -W.; Kettrup, A.; Schlag, E. W. *Chemosphere* **1994**, *29*, 1429-1440.
13. Matsui, T.; Fukazawa, K.; Fujimoto, M.; Imasaka, T. *Anal. Sci.* **2012**, *28*, 445-450.
14. Li, A.; Imasaka, T.; Uchimura, T.; Imasaka, T. *Anal. Chim. Acta* **2011**, *701*, 52-59.

15. Hamachi, A.; Okuno, T.; Imasaka, T.; Kida, Y.; Imasaka, T. *Anal. Chem.* **2015**, *87*, 3027-3031.

16. Ledingham, K. W. D.; Singhal, R. P. *Int. J. Mass Spectrom.* **1997**, *163*, 149-168.

17. Imasaka, T. *Anal. Bioanal. Chem.* **2013**, *405*, 6907-6912.

18. Tang, Y.; Imasaka, T.; Yamamoto, S.; Imasaka, T. *Chemosphere* **2016**, *152*, 252-258.

19. Shibuta, S.; Imasaka, T.; Imasaka, T. *Anal. Chem.* **2016**, *88*, 10693-10700.

20. Palit, M.; Gupta, A. K.; Jain, R.; Raza, S. K. *J. Chromatogr. A* **2004**, *1043*, 275-284.

21. Hashiguchi, Y.; Zaitsu, S.; Imasaka, T. *Anal. Bioanal. Chem.* **2013**, *405*, 7053-7059.

22. Imasaka, T.; Imasaka T. *Anal. Sci.* **2014**, *30*, 1113-1120.

23. Becke, A. D. *J. Chem. Phys.* **1993**, *98*, 5648-52.

24. Dunning Jr., T. H. *J. Chem. Phys.* **1989**, *90*, 1007-23.

25. Kendall, R. A.; Dunning Jr., T. H.; Harrison, R. J. *J. Chem. Phys.* **1992**, *96*, 6796-6806.

26. Bauernschmitt, R.; Ahlrichs, R. *Chem. Phys. Lett.* **1996**, *256*, 454-64.

27. Richardson, D. D.; Caruso, J. A. *Anal. Bioanal. Chem.* **2007**, *388*, 809-823.

28. Purdon, J. G.; Pagotto, J. G.; Miller, R. K. *J. Chromatogr.* **1989**, *475*, 261-272.

29. Kouno, H.; Imasaka, T. *Analyst* **2016**, *141*, 5274-5280.

30. Amirav, A.; Gordin, A.; Poliak, M.; Fialkov, A. B. *J. Mass Spectrom.* **2008**, *43*, 141-163.

Figure Captions

Fig. 1 (A) Metabolic pathway of sarin and soman. IMPA, isopropyl methylphosphonic acid; PMPA, pinacolyl methylphosphonic acid; MPA, methylphosphonic acid. (B) Derivatization of IMPA and PMPA. PFB, 2,3,4,5,6-pentafluorobenzyl group.

Fig. 2 Calculated absorption spectra for (A) IMPA-PFB and (B) PMPA-PFB. *EE*, the lowest transition energy; *IE*, ionization energy; *IE*/2, half of the ionization energy.

Fig. 3. (A) (C) mass spectra and (B) (D) mass chromatograms measured for IMPA-PFB at 352 s and m/z = 318, respectively. Laser wavelength: (A) (B) 267 nm (C) (D) 200 nm. Sample concentration, 100 ng/mL. Peak assignments are shown in the figure.

Fig. 4. Expanded view of the two-dimensional display measured for IMPA-PFB. Laser wavelength, (A) 267 nm (B) 200 nm. Sample concentration, 100 ng/mL. The signal for the molecular ion is indicated by a circle (pink) in the figure.

Fig. 5. (A) (C) mass spectra and (B) (D) mass chromatograms measured for PMPA-PFB at 415 s and m/z = 360, respectively. Laser wavelength: (A) (B) 267 nm (C) (D) 200 nm. Sample concentration, 100 ng/mL. Assignments of the signal peaks are shown in the figure. Two peaks are observed for PMPA-PFB (explained in the text). An expanded view is shown as an insert in the figure.

Fig. 6. Expanded view of the two-dimensional display measured for PMPA-PFB at 200 nm. (A) mass chromatogram measured at m/z = 360 (B) mass spectrum measured at 415 s. Sample concentration, 100 ng/mL. The baseline level (blue plane) in the two-dimensional display was adjusted to isolate the molecular ion peaks. In fact, major parts of the signals in the GC shown in (A) originate from the background arising from the fragment signals, even when the signal was monitored at m/z = 360 (explained in the text).

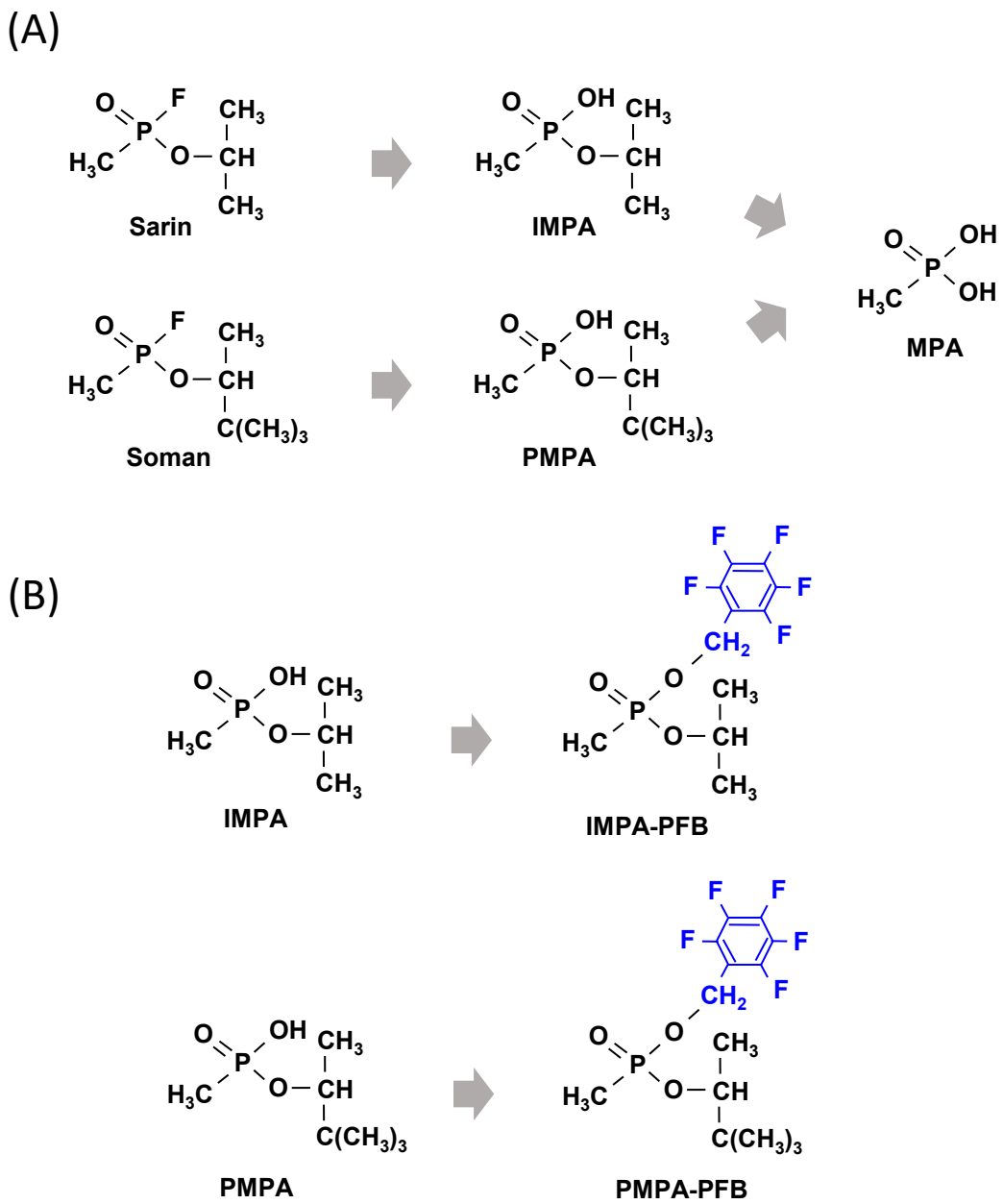

Fig. 1 A. Hamachi et al.

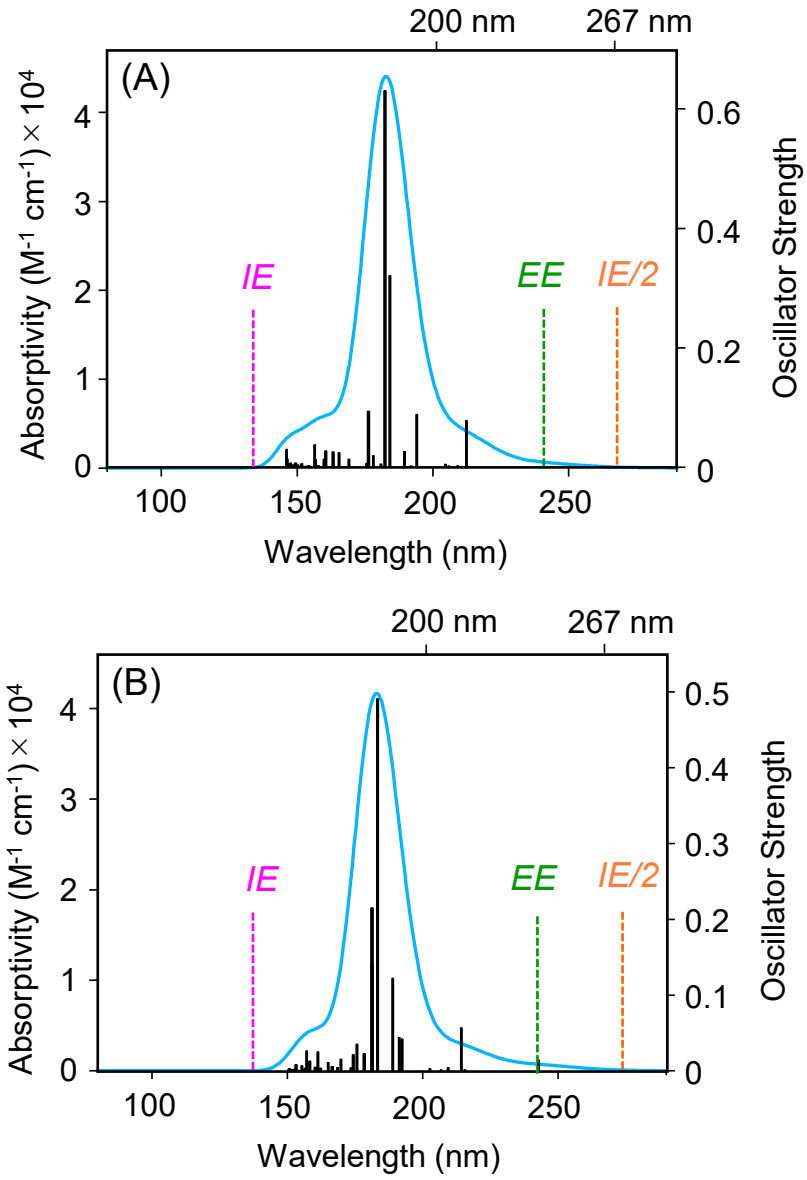

Fig. 2 A. Hamachi et al.

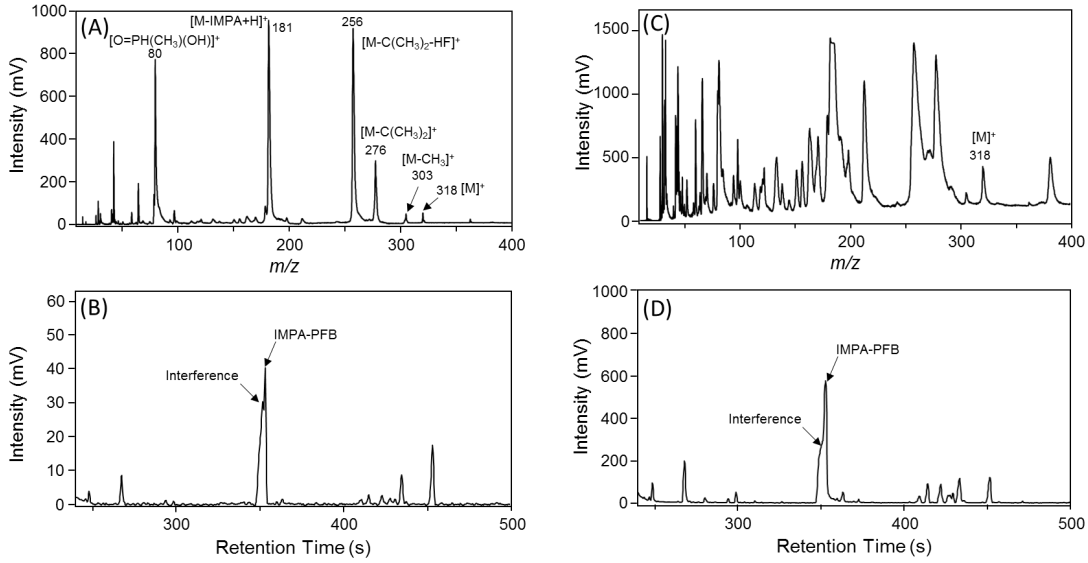

Fig. 3 A. Hamachi et al.

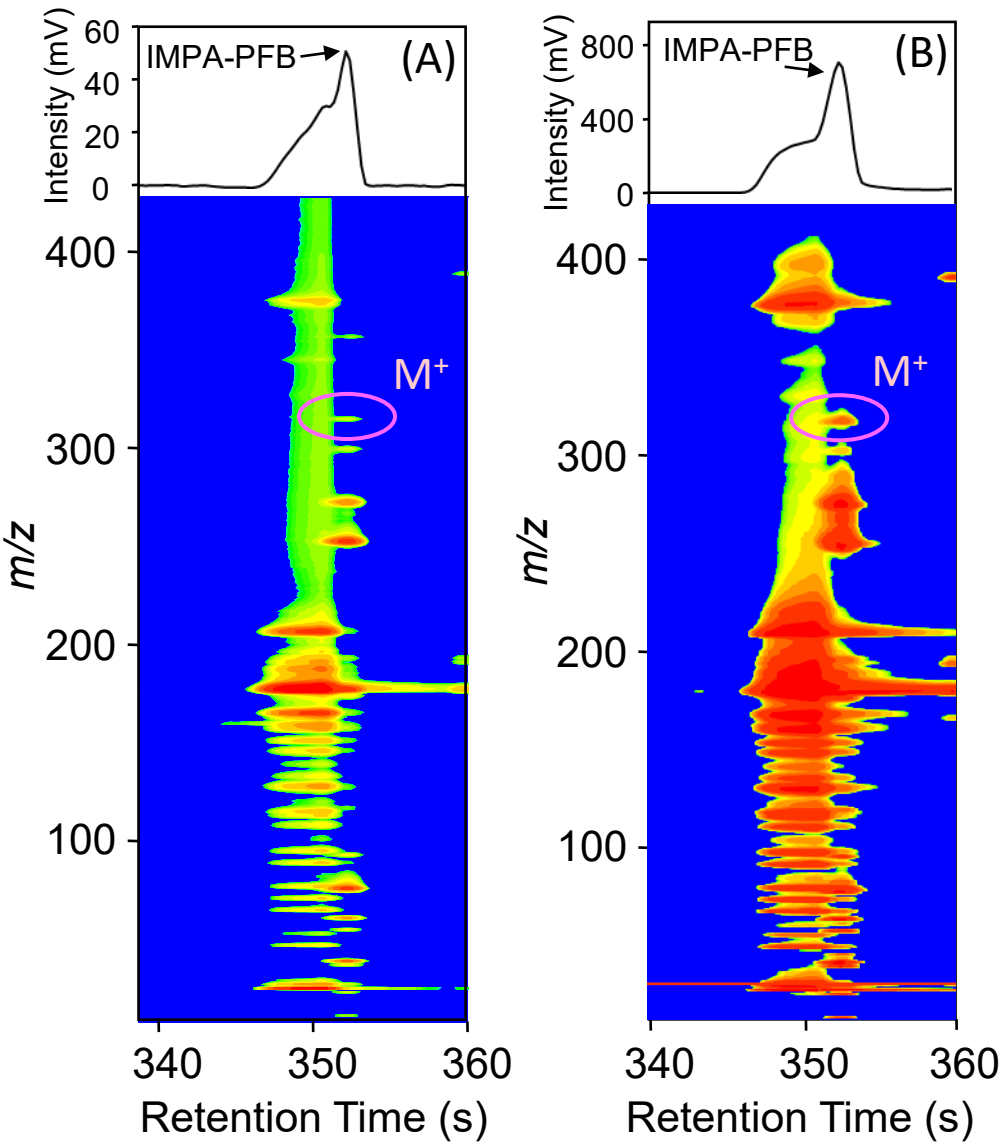

Fig. 4 A. Hamachi et al.

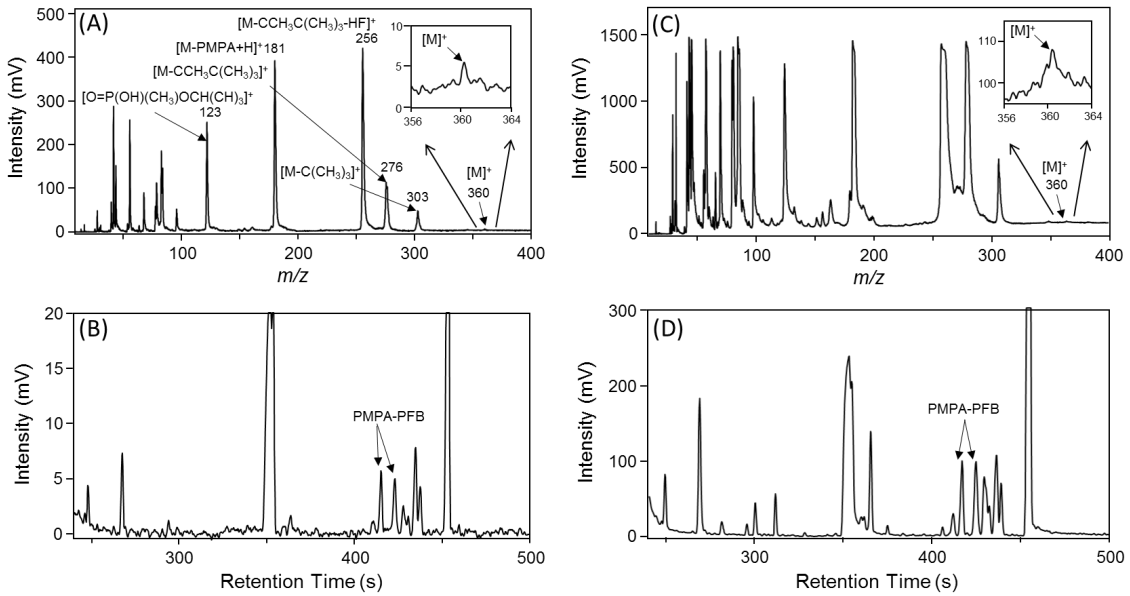

Fig. 5 A. Hamachi et al.

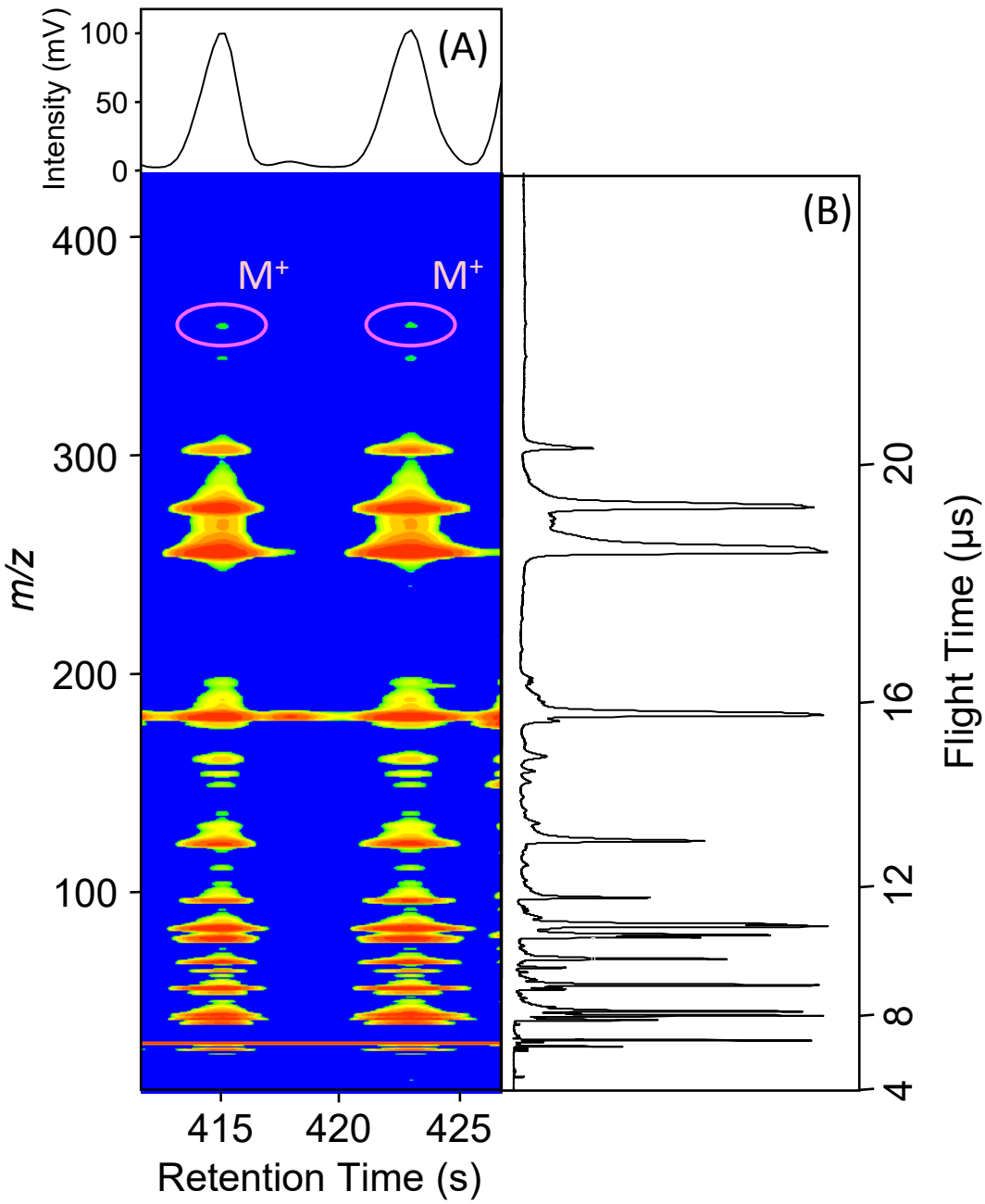

Fig. 6 A. Hamachi et al.